# Spectral, Thermal, Crystal Structure, Hirshfeld Surface Analyses and Biological Activities of New Hydrazinium Dipicolinato Copper(II) Tetrahydrate

K. Naresh and B.N. Sivasankar[*]

Department of Chemistry, Government Arts College, Udhagamandalam, The Nilgiris-643002, India

*Corresponding author: E-mail: sivabickol@yahoo.com

A new copper complex of pyridine-2,6-dicarboxylate containing hydrazinium cation, formulated as $(N_2H_5)_2[Cu(PDC)_2]\cdot4H_2O$ (PDC = pyridine-2,6-dicarboxylate) has been synthesized from copper(II) nitrate, hydrazine hydrate and pyridine-2,6-dicarboxylic acid as a single crystal and characterized by elemental analysis and spectroscopic (IR and UV-visible), thermal (TG/DTG), single crystal X-ray diffraction and biological studies. A six-coordinate complex with a distorted octahedral geometry around Cu(II) ion is proposed and confirmed by X-ray single crystal method. The structure reveals that two pyridine-2,6-dicarboxylate species acting as tridentate ligands and hydrazinium cation present as a counter ion along with non-coordinated four water molecules. The structural units of copper(II) is mutually held by the hydrogen bonds and π···π and C–O···π interactions. The copper(II) complex is connected to one another *via* O–H···O hydrogen bonds, forming water clusters, which plays an important role in the stabilization of the crystal structure. In the water clusters, the water molecules are trapped by the cooperative association of coordination interactions as well as hydrogen bonds. Both cation and anion interactions and crystal from various types of intermolecular contacts and their importance were explored using Hirshfeld surface analysis. This indicates that O···H/H···O interactions are the superior interactions conforming excessive H-bond in the molecular structure. The interaction of copper(II) complex with calf thymus DNA (CT-DNA) was investigated by electronic absorption spectroscopic technique. The electronic evidence strongly shows that the compound interacts with calf thymus through intercalation with a binding constant of $K_b = 5.7 \times 10^4$ M$^{-1}$.

**Keywords: Tridentate, Single crystal, Biological studies, Hirshfeld surface analysis, DNA binding studies.**

## INTRODUCTION

Many transition and heavy metal cations play an active role in the great number of various biological processes, being a component of several vitamins and drugs. Pyridine-2,6-dicarboxylic acid and their derivatives are interesting series of compounds with biological applications [1]. The metal carboxylates are very interesting as the carboxylate ion can coordinate to the metal as unidentate, chelating or bridging ligand [2]. Moreover pyridine-2,6-dicarboxylate (PDC) can act as N-donor ligand due to the presence of pyridine nitrogen atom in addition to their carboxylate O-donor ability [3]. Copper(II) carboxylates exhibit diverse structures due to the various coordination modes of the carboxylato ligand [4]. Metals in multinuclear complexes allows the design of new materials with useful magnetic and electronic properties [5]. Both pyridine and carboxylate func-

tionalities give these ligands versatile coordination modes towards different metal ions [6,7]. Polycarboxylates attracted interest as potential bridging ligands towards transition metal centers with abundant structural motifs [8]. A polymeric structure of PDC complexes with transition and lanthanide metals has been reported in which PDC not only chelates but also bridges to form diversified structures [9].

Most of the complexes contain deprotonated anion (PDC), whereas monodeprotonated HPDC⁻ forms complexes with Co(II), Ni(II), Cu(II) and Zn(II) [10]. A copper(II) complex containing one unit of protonated $H_2PDC$ and one unit of double protonated PDC was synthesized [11]. $H_2PDC$ and its anion (HPDC⁻, PDC) have proved good candidates for the construction of supermolecular assemblies, because they exhibit diverse coordination modes and also function as hydrogen-bond acceptors as well as the hydrogen-bond donor. Dipicolinic acid is

one of the most suitable ligand systems for modeling potential of the low toxicity, amphophilic nature and biological activities [12]. Dipicolinic acid has the ability of ligand to give suitable chelates with different coordination modes and has the ability to form strong hydrogen bond and it is biological active in human metabolism [13,14]. Although lots of dipicolinate complexes of transition metals are known and hetero binuclear pyridine-2,6-carboxylate complexes are limited.

Hydrazine is a weaker base than ammonia, still it is capable of replacing two protons from the $H_2PDC$ and capable of forming monohydrazinium salts [15]. It has two nitrogen atoms with lone pairs, but only one lone pair was utilized during the formation of hydrazinium salts. The other lone pair is available is exploited for coordination of hydrazinium cation with several metal ions in the presence of anions such as fluoride, chloride, thiocyanide, sulfite and simple and substituted carboxylates and dicarboxylates [16]. In this article, we wish to report the structure of a new hydrazinium copper(II) dipicolinate tetrahydrate complex, which shows some salient features that are not observed in any of the metal-PDC complexes reported so far.

## EXPERIMENTAL

All the chemicals used were of AnalaR or equivalent grade. The chemicals were used as received from S.D. Fine chemicals. The hydrazine content was determined volumetrically using a 0.025 M $KIO_3$ solution under Andrew's condition [17]. The metal content was determined by EDTA complexometric titration [18]. The C, H and N analyses were carried out using a Perkin-Elmer (model 1240) CHN elemental analyzer. UV-visible absorbance spectrum was recorded on Systronics double beam 2022 spectrophotometer in the range 800-200 nm. FT-IR spectrum was obtained with KBr pellets on a Perkin-Elmer 597 spectrophotometer in the range of 4000-400 $cm^{-1}$. The simultaneous TG-DTA analysis was carried out on a SWITG/DTA 6200 thermal analyzer under air from 0-800 °C and the heating rate employed was 10 °C $min^{-1}$ using 5 mg of the sample and aluminium cups as sample holders. X-ray single crystal data of the complex was collected using Enraf-Nonius CAD-4 diffractometer with Mo-$K_\alpha$ radiation ($\lambda$ = 0.71073 Å) and graphite as a monochromator. The structures were solved by the Patterson method and refined by applying full matrix least square techniques. Refinements were carried out using SHELEX-97 program [19,20]. Atomic scattering factors and anomalous dispersion collections were obtained from international data for X-ray crystallography [21]. The structure model was drawn using ORTEP.

**Hirshfeld surface analysis:** Molecular Hirshfeld surface calculations of copper(II) complex was performed by using the Crystal Explorer 3.1 program [22]. Hirshfeld surfaces [23,24] and the associated two-dimensional (2D) fingerprint plots were calculated using crystal explorer [25,26], with bond lengths to hydrogen atoms set to standard values [27].

**Biological screening:** The antibacterial and antifungal testing of the copper(II) complex was performed by the procedure described in the literature [28]. The antiviral activity of the complex was tested at JSS College of Pharmacy, Udhagamandalam, The Nilgiris, India. The procedure for the antiviral testing is similar to that described the literature [29]. The

copper(II) complex was screened *in vitro* for their biological activity by using bacteria, namely *Escherichia coli*, *Pseudomonas aeruginosa*, Methicillin-resistant *Staphylococcus aureus*, *Bacillius subtilis* and fungi, namely *Aspergillus niger*, *Candida albicans* by the reported method [30]. Sterile nutrient agar plates were prepared by pouring the sterile agar into sterile petri dishes under aseptic condition. 0.1 mL of the test organism was spread on agar plates. 5 mm diameter holes were made in the agar plates using a sterile bore. Drug as well as the standard drug and the DMSO solvent control were added into each hole separately. The plates were maintained at 4 °C for 1 h to allow the diffusion of solution into the agar medium. All the plates containing bacteria were incubated at 37 °C for 24 h and that of fungi at 28 °C for 48 h.

**DNA binding studies:** The binding affinity with CT-DNA was carried out in double distilled water as a buffer containing 5 mm *tris*(hydroxyl-methyl)ammomethane and 50 mM sodium chloride, pH is adjusted to 7.2 with hydrochloric acid, 1.8-1.9 at 200-350 nm, indicating the DNA was sufficiently free of protein [31]. The DNA concentration per nucleotide was determined by absorption spectroscopy using the molar extinction coefficient value of 6600 $dm^3$ $mol^{-1}$ $cm^{-1}$ at 260 nm [32]. The compound was dissolved with 5 % water and 95 % of *tris*-HCl buffer for the experiments. Stock solutions were stored at 4 °C and used within 4 days. Absorption titration experiments were performed with a fixed concentration of the complex (5 μM) and varying concentration of DNA (0-25 μM). While measuring the electronic absorption spectra, an equal amount of DNA was added to the test solutions and the reference solution to eliminate the electronic absorbance of DNA itself [33].

**Synthesis of complex:** A solution of pyridine-2,6-dicarboxylic acid (3.26 g, 0.02 mol) in water (25 mL) was neutralized with hydrazine hydrate (2.00 mL, 0.04 mol). This mixture was added to an aqueous solution (30 mL) of $Cu(NO_2)_3 \cdot 3H_2O$ (2.91 g, 0.01 mol) with stirring. The resulting solution was stirred well and the excess of acid precipitated was removed. The clear solution was concentrated to one third of its original volume. After cooling to room temperature the clear solution was allowed to crystallize and the blue crystals formed after 2-3 days were collected, washed quickly with ice cold water and dried in air. Yield: 53.4 %.

## RESULTS AND DISCUSSION

Dihydrazinium *bis*(pyridine-2,6-dicarboxylate) copper(II) tetrahydrate was isolated as a single crystal from the aqueous solution containing a mixture of hydrazine hydrate, $H_2PDC$ and copper(II) nitrate trihydrate. The complex is blue in colour, soluble in water and stable in air. The chemical analyses show that the composition is $(N_2H_5)[Cu(PDC)_2] \cdot 4H_2O$. The analytical data is given below: $C_{14}H_{24}CuN_6O_{12}$: Calc. $N_2H_4$, 12.41; Cu, 12.13; C, 31.60; H, 4.54; N, 15.80 %; Found: $N_2H_4$, 11.78; Cu, 11.84; C, 30.98; H, 4.69; N, 15.38 %.

**Electronic spectrum:** The UV-visible spectrum of $(N_2H_5)_2[Cu(PDC)_2] \cdot 4H_2O$ in water was measured at room temperature. The copper(II) complex show a higher energy band at 13,888 cm for the transition from $B_1(d_{x^2-y^2})$ ground to excited $A_1(d_{z^2})$, $B_2(d_{xy})$ and $E(d_{xz}, d_{yz})$ states. This step occurs at *d-d* transition. Two bands occur in lower energy at 27,777

cm is attributed to the intra ligand $\pi{\rightarrow}\pi^*$ and $n{\rightarrow}\pi^*$ charge transfer transitions (ILCT) respectively [34].

**Infrared spectra:** The IR spectrum of the complex (Fig. 1) shows a broad band in the region between 3600-3200 cm⁻¹ respectively, which are assigned to N-H and O-H stretching of hydrazine and water molecules. The N-N stretching of hydrazinium cation is observed as a sharp band at 975 cm⁻¹ which supports the ionic nature $N_2H_5^+$ ion [35]. The pyridine ring exhibit bands in the range of 760-690 cm⁻¹. Two bands observed at 1620 and 1380 cm⁻¹ are assigned to $\nu_{asy}$ and $\nu_{sym}$ stretchings of carboxylate ion with $\Delta\nu = 240$ cm⁻¹ corresponds to monodentate coordination [36].
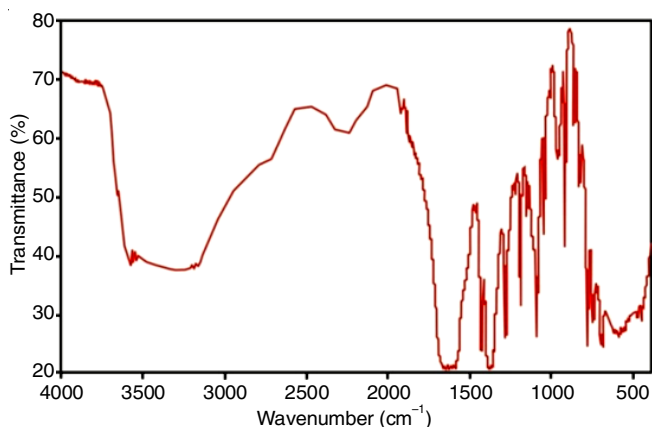


Fig. 1. IR spectrum of $(N_2H_5)_2[Cu(PDC)_2]\cdot 4H_2O$

**Thermal degradation:** The simultaneous TG-DTA of copper(II) complex proceeds in three stages (Fig. 2). In the first step, (100-180 °C) loss of lattice water molecule takes place which is associated (endothermic) with 13.54 % weight loss which is close to the theoretical value of 14 %. The higher dehydration temperature could be due to the strong hydrogen bonding interaction. In the second step, two hydrazinium molecule are eliminated in the temperature range between 180-350 °C to yield $Cu(HPDC)_2$ as the intermediate. The third step intermediate $Cu(HPDC)_2$ further undergoes pyrolysis to yield
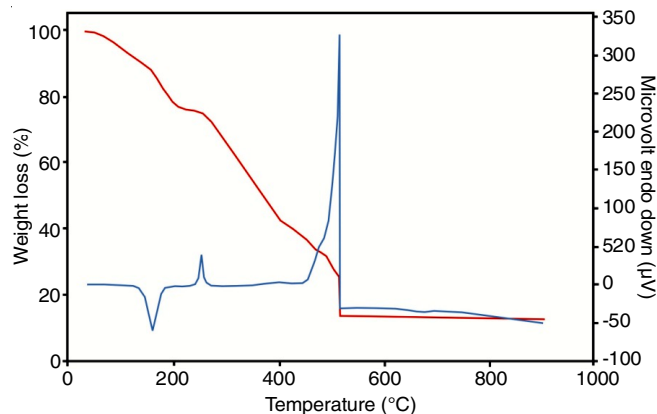


Fig. 2. Simultaneous TG-DTA of $(N_2H_5)_2[Cu(PDC)_2]\cdot 4H_2O$

CuO as a final residue. TG show 87.91 % weight loss and DTA shows a sharp exotherm at 510 °C to this stage.

**Crystal structure of $(N_2H_5)_2[Cu(PDC)_2]\cdot 4H_2O$:** The complex crystallizes in a monoclinic crystal system with $P2_1/n$ space group. There are four water molecules present in the unit cell and the observed density, 1.6 mg/m³ is very close to that of the calculated value of 1.638 mg/m³. A small variation in the N-N bond length of two hydrazinium cation observed could be due to the slightly different environment and interaction. The crystal structure shows that there are three discrete ions present in the system, two $N_2H_5^+$ ions and one $[Cu(PDC)^{2-}]^{2+}$ cation along with four lattice water molecules.

The ORTEP view and packing diagram of the complex are shown in Fig. 3a and 3b, respectively. The structure clearly reveals that the Cu(II) ion is surrounded by two tridentate pyridine-2,6-dicarboxylate dianions resulting in the slightly distorted octahedral structure. The ligand binds in [N,O,O] chelating fashion. Thus the central metal ion surrounded by four oxygen atoms O1, O3, O5 and O7 and two tertiary nitrogen atoms N1 and N2. Two oxygen atoms such as O1 and O3 and two tertiary nitrogen atoms comprise the equatorial position while the two other oxygen atoms O5 and O7 occupy the axial position. The bond lengths of Cu-O5 (2.2456 Å) and Cu-O7
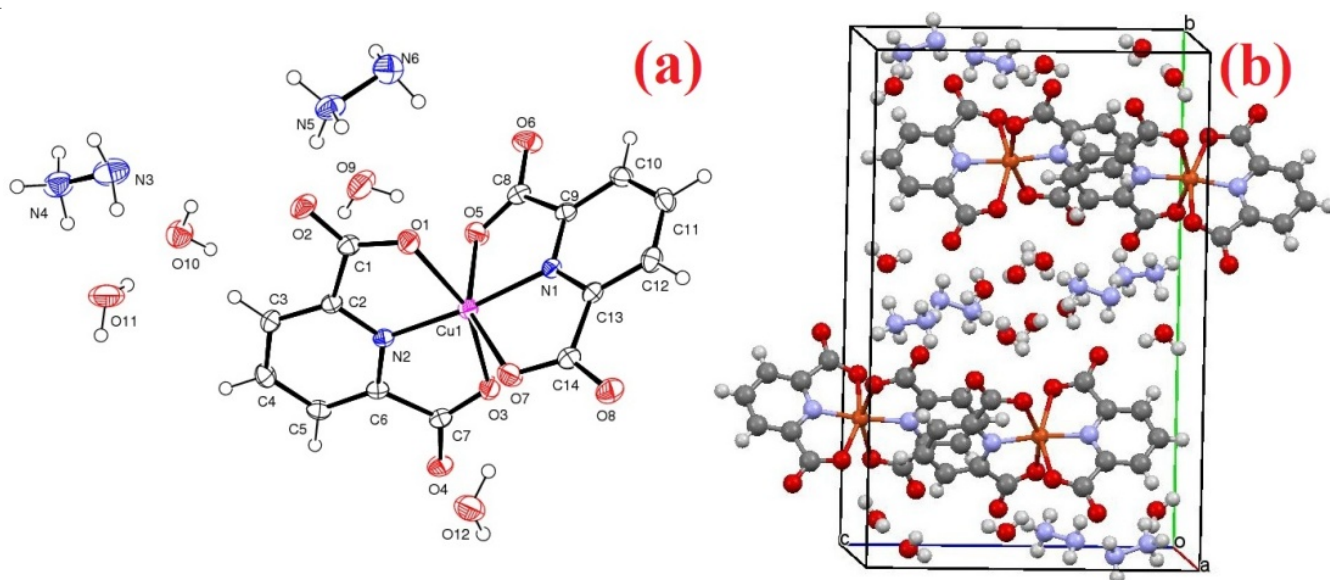


Fig. 3. (a) ORTEP plot of $(N_2H_5)_2[Cu(PDC)_2]\cdot 4H_2O$, 4 (b) Packing diagram of $(N_2H_5)_2[Cu(PDC)_2]\cdot 4H_2O$

(2.2818 Å) are longer than Cu-N1 (1.9435 Å), Cu-N2 (1.9140 Å), Cu-O1 (2.1299 Å) and Cu-O3 (2.1523 Å) due to the john teller effect [37]. The selected bong lengths, bond angles and intermolecular hydrogen bond data are summarized in Tables 1-3, respectively. Two carboxylate groups from the one PDC

### TABLE-1
### CRYSTAL DATA AND STRUCTURE REFINEMENT FOR $(N_2H_5)_2[Cu(PDC)_2] \cdot 4H_2O$

| | |
|---|---|
| CCDC No | 1886936 |
| Formula weight | 531.93 |
| Temperature | 296(2) K |
| Wavelength | 0.71073 Å |
| Crystal system | Monoclinic |
| Space group | $P2_1/n$ |
| Unit cell dimensions | a = 7.9280(3) Å; $\alpha = 90°$ |
| | b = 20.6145(7) Å; $\beta = 92.5390(10)°$ |
| | c = 13.2129(5) Å; $\gamma = 90°$ |
| Volume | 2157.29(14) Å$^3$ |
| Z | 4 |
| Density (calculated) | 1.638 Mg/m$^3$ |
| Absorption coefficient | 1.087 mm$^{-1}$ |
| F(000) | 1100 |
| Crystal size | 0.150 × 0.100 × 0.100 mm$^3$ |
| Theta range for data collection | 1.832 to 24.999° |
| Index ranges | -9<=h<=9, -24<=k<=24, -15<=l<=15 |
| Reflections collected | 26074 |
| Independent reflections | 3797 [R(int) = 0.0282] |
| Completeness to $\theta$ = 24.999° | 100.0 % |
| Absorption correction | Semi-empirical from equivalents |
| Max. and min. transmission | 0.7462 and 0.6971 |
| Refinement method | Full-matrix least-squares on F$^2$ |
| Data/restraints/parameters | 3797/30/370 |
| Goodness-of-fit on F$^2$ | 1.027 |
| Final R indices [I>2σ(I)] | R1 = 0.0264, wR2 = 0.0703 |
| R indices (all data) | R1 = 0.0332, wR2 = 0.0748 |
| Extinction coefficient | n/a |
| Largest diff. peak and hole | 0.288 and -0.424 e.Å$^{-3}$ |

### TABLE-2
### BOND LENGTHS (Å) AND ANGLES (°) OF $(N_2H_5)_2[Cu(PDC)_2] \cdot 4H_2O$

| Bond lengths (Å) | | | |
|---|---|---|---|
| N(1)-Cu(1) | 1.9435(16) | O(1)-Cu(1) | 2.1299(14) |
| N(2)-Cu(1) | 1.9140(16) | O(3)-Cu(1) | 2.1523(14) |
| N(3)-N(4) | 1.444(3) | O(5)-Cu(1) | 2.2456(15) |
| N(5)-N(6) | 1.435(3) | O(7)-Cu(1) | 2.2818(14) |

| Angles (°) | | | |
|---|---|---|---|
| C(9)-N(1)-Cu(1) | 118.12(13) | N(6)-N(5)-H(5C) | 108.8(18) |
| C(13)-N(1)-Cu(1) | 121.27(13) | N(5)-N(6)-H(6A) | 107(2) |
| C(2)-N(2)-Cu(1) | 118.41(13) | N(5)-N(6)-H(6B) | 100(2) |
| C(6)-N(2)-Cu(1) | 120.16(13) | C(1)-O(1)-Cu(1) | 112.52(12) |
| N(4)-N(3)-H(3A) | 107(2) | C(7)-O(3)-Cu(1) | 113.51(12) |
| N(4)-N(3)-H(3B) | 104.2(19) | C(8)-O(5)-Cu(1) | 109.89(12) |
| N(3)-N(4)-H(4A) | 107.9(17) | C(14)-O(7)-Cu(1) | 111.85(12) |
| N(3)-N(4)-H(4B) | 108.9(16) | N(2)-Cu(1)-N(1) | 173.47(6) |
| N(3)-N(4)-H(4C) | 112.8(18) | N(2)-Cu(1)-O(1) | 79.39(6) |
| N(6)-N(5)-H(5A) | 114.5(16) | N(1)-Cu(1)-O(1) | 96.02(6) |
| N(6)-N(5)-H(5B) | 108.5(15) | N(2)-Cu(1)-O(3) | 78.33(6) |

Symmetry transformations used to generate equivalent atoms.

ion contribute two oxygen atoms for the coordination which are in the axial position. Two other oxygen atoms from second PDC ring are in the same plane of the square planar arrangement around the metal ion. The first PDC ion is perpendicular to this plane (Fig. 3a). The distance between PDC rings in the neighboring molecules is 3.851 Å which is due to π-π stacking. This interaction has been considered as an effective factor on the stability of biological and chemical system. The hydrogen bonding interaction also plays an important role in the stabilization of the crystal structure. In the present system, four water molecules are involved in the hydrogen bonding with carboxylate oxygen atoms.

Two hydrazinium cations are capable of coordination with Cu(II) ions. Since PDC ion from strong chelating rings with metal ion the hydrazinium cation is present outside the coordination sphere as charge neutralizing species. These cations

### TABLE-3
### HYDROGEN BONDS OF $(N_2H_5)_2[Cu(PDC)_2] \cdot 4H_2O$ (Å and °)

| D-H···A | d(D-H) | d(H···A) | d(D···A) | ∠(DHA) |
|---|---|---|---|---|
| C(5)-H(5)···O(1)#1 | 0.93 | 2.63 | 3.520(2) | 160.4 |
| C(10)-H(10)···O(12)#2 | 0.93 | 2.39 | 3.294(3) | 165.4 |
| N(3)-H(3A)···O(8)#3 | 0.882(17) | 2.238(19) | 3.099(3) | 165(3) |
| N(3)-H(3B)···O(6)#4 | 0.898(16) | 2.161(17) | 3.058(3) | 179(3) |
| N(4)-H(4A)···O(11) | 0.918(15) | 1.826(15) | 2.722(3) | 165(3) |
| N(4)-H(4B)···O(4)#5 | 0.899(15) | 1.954(15) | 2.827(2) | 163(2) |
| N(4)-H(4C)···O(12)#6 | 0.907(15) | 1.881(15) | 2.773(3) | 167(3) |
| N(5)-H(5A)···O(2) | 0.921(15) | 1.869(15) | 2.782(2) | 170(2) |
| N(5)-H(5B)···O(6)#7 | 0.912(15) | 1.842(15) | 2.729(2) | 164(2) |
| N(5)-H(5C)···O(9)#4 | 0.923(15) | 1.889(17) | 2.772(3) | 160(2) |
| N(6)-H(6A)···O(2)#4 | 0.873(16) | 2.262(19) | 3.052(3) | 151(3) |
| N(6)-H(6B)···O(4)#8 | 0.869(17) | 2.34(2) | 3.072(3) | 142(3) |
| O(9)-H(9A)···O(5) | 0.837(17) | 1.964(18) | 2.795(2) | 172(3) |
| O(9)-H(9B)···O(8)#1 | 0.844(18) | 2.024(18) | 2.860(3) | 171(4) |
| O(10)-H(10A)···O(8)#1 | 0.823(16) | 2.042(18) | 2.855(2) | 170(3) |
| O(10)-H(10B)···N(6)#4 | 0.825(16) | 2.065(17) | 2.890(3) | 179(3) |
| O(11)-H(11A)···O(10) | 0.826(17) | 1.978(17) | 2.770(3) | 161(3) |
| O(11)-H(11B)···O(3)#3 | 0.823(16) | 1.913(17) | 2.734(2) | 174(3) |
| O(12)-H(12A)···O(7) | 0.831(16) | 1.966(17) | 2.775(2) | 164(3) |
| O(12)-H(12B)···O(10)#9 | 0.829(17) | 2.050(17) | 2.857(3) | 165(3) |

Symmetry transformations used to generate equivalent atoms: #1 x+1/2,-y+1/2,z+1/2; #2 x+1/2,-y+1/2,z-1/2; #3 x-1/2,-y+1/2,z+1/2; #4 -x+1, -y,-z+1; #5 -x+3/2,y-1/2,-z+3/2; #6 -x+1/2,y-1/2,-z+3/2; #7 x-1,y,z; #8 x-1/2,-y+1/2,z-1/2; #9 -x+3/2,y+1/2,-z+3/2

are also involved in the hydrogen bonding interaction with water molecules and ligand molecules.

**Hirshfeld surface analysis:** Hirshfeld surface depends on the geometry of the molecules, orientation of the molecules in the neighbourhood and the nature of atoms that make close contacts in the chosen molecule. The $d_{norm}$, $d_e$, $d_i$, curvedness and shape index of copper(II) complex are shown in Fig. 4. The $d_{norm}$ surface shows intermolecular contacts relative to the van der Waals radius by way of a simple red (higher electron density) and blue (lower electron density) colour design. The $d_{norm}$, $d_e$ and $d_i$ of copper(II) complex shown in red colour on carboxylate and N-H groups. The curvedness and shape index are measurements of curvature (flat region) and shape (triangle) of Hirshfeld surface respectively. The curvedness of copper(II) complex consists of green flat region and blue outline. The shape index is the meaurement of shape in Hirshfeld surfaces. Curvedness and shape index confirm the contacts between neighbouring molecules.

The percentages of contacts by way of 2D fingerprint plots of copper(II) complex are shown in Fig. 4. From the analysis, it is found that the O···H interaction is the most outstanding interaction in the total Hirshfeld area for copper(II) complex that amounts to 47.6 %. The H···H interactions are reflected in the middle of 2D fingerprint plots as scattered points which contribute to only 30.6 % of the total Hirshfeld surfaces. The O···H contacts are due to both N-H···O and C-H···O interactions. The red spots on the Hirshfeld surfaces correspond to the N-H···O hydrogen bond interactions whereas the blue areas and the green areas correspond to π-π interactions and the H···H contacts respectively. The O···H, H···H and O···O interactions arise from N-H···O, O-H···O and C-H···O hydrogen bonds in copper(II) as shown in the $d_{norm}$ surface. The C···C (6.0 %), N···H (5.9 %), C···H (5.7 %) interactions observed in copper(II) amounts to only a small fraction of the Hirshfeld surface. This small value is an indicator of absence of N-C···H hydrogen bonding. The higher % of O···H contacts is responsible for the supramolecular architecture and variety of hydrogen bonding interactions (Fig. 5).
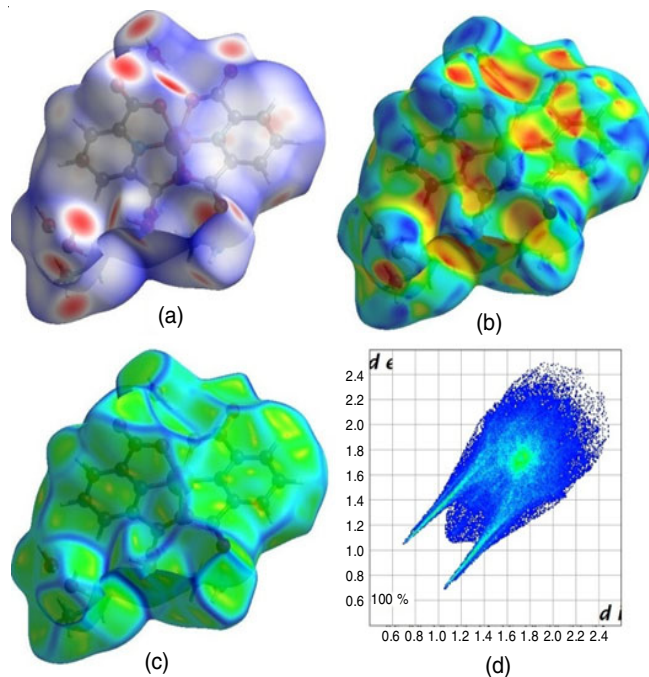


Fig. 4. (a) $d_{norm}$ (b) Shape index (c) Curvedness on the Hirshfeld surface intermolecular forces belong the title compound and (d) 2D fingerprint 100 %

***in vitro* Antibacterial and antifungal assay:** The antibacterial and antifungal activity data of copper(II) complex are shown in Table-4. The copper(II) complex was screened for their bacterial activity against *Escherichia coli*, *Pseudomonas aeruginosa*, Methicillin-resistant *Staphylococcus aureus*, *Bacillus subtilis*. Copper(II) complex was more active against *Escherichia coli*, *Pseudomonas aeruginosa* and inactive against Methicillin-resistant *Staphylococcus aureus* and *Bacillus subtilis* [38].

Antifungal screening of copper(II) complex was carried against *Aspergillus niger* and *Candida albicans* fungal strains and compared with the standard drug. These results revealed that the complex is more active against *Aspergillus niger* and inactive against *Candida albicans* [39].
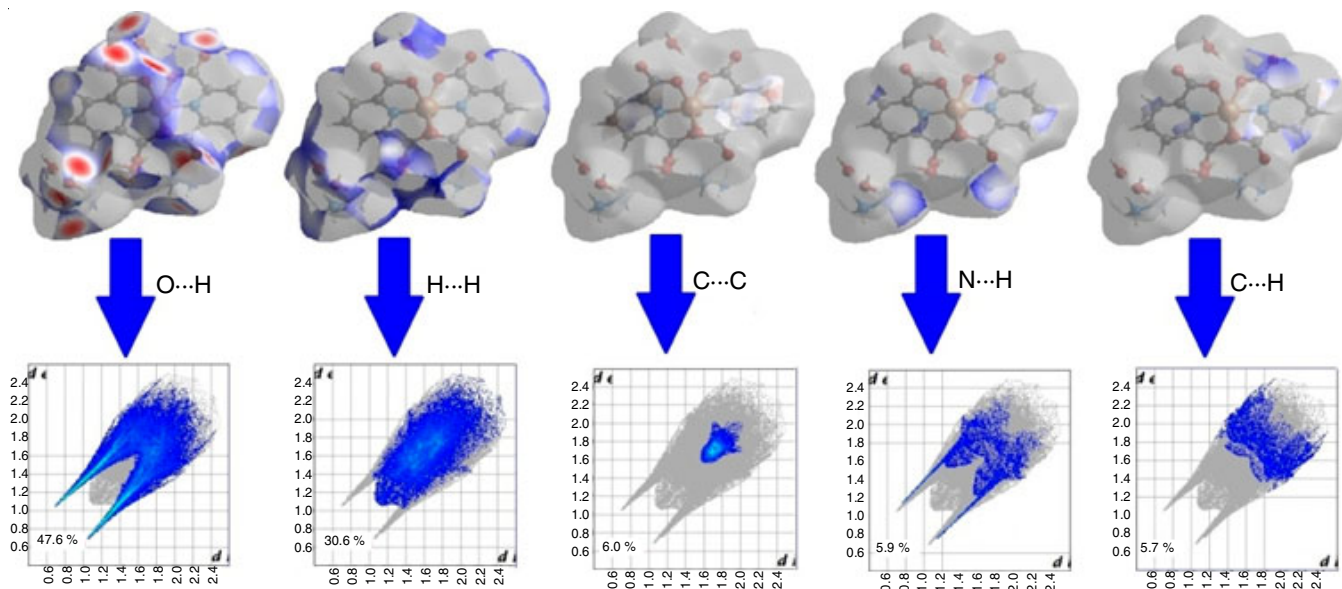


Fig. 5. Two dimensional fingerprint plot with a $d_{norm}$ view

| Conc. (µg mL⁻¹) | Zone of inhibition (%) | | | | | |
|---|---|---|---|---|---|---|
| | Antibacterial activity | | | | Antifungul activity | |
| | *E. coli* | *P. aeruginosa* | MRSA | *B. subtilis* | *A. niger* | *C. albicans* |
| 1 | 16 | 16 | – | – | 17 | – |
| 2 | 16 | 15 | – | – | 18 | – |
| 3 | 18 | 17 | – | – | 21 | – |
| 4 | 15 | 15 | – | – | 19 | – |

## DNA binding studies

**Electronic absorption titration:** Electronic absorption spectroscopy is effective method to examine the binding modes of metal complexes with DNA. Compound binding through intercalation usually results in hypochromism with or without small blue and red shift. The intercalative modes involve a strong interaction of DNA [40]. The electronic absorption spectra of compound in the absence and presence of CT-DNA are given in Fig. 6. The electronic absorption spectroscopy revealed the shift in the wavelength as a function of concentration of DNA. It confirms the binding of the compound with DNA. Addition of increased amount of CT-DNA shows significant hypochromism and red shift of 3-5 nm is observed in the band at 200-350 nm. The electronic absorption data were analyzed to evaluate the intrinsic binding constant ($K_b$), which can be determined from the following equation [41].

$$[DNA]/(\varepsilon_a - \varepsilon_f) = [DNA]/(\varepsilon_b - \varepsilon_f) + 1/K_b(\varepsilon_b - \varepsilon_f)$$

where, [DNA] is the concentration of DNA absorption coefficient $\varepsilon_a$, $\varepsilon_b$, $\varepsilon_f$ corresponds to $A_{obs}$/[compound] the extinction coefficient of free compound and the extinction coefficient of the compound fully bound to DNA respectively. From the plot of $[DNA]/(\varepsilon_a - \varepsilon_f)$ *versus* DNA, $K_b$ is calculated by the ratio of slope of the intercept. The magnitude of intrinsic binding constant ($K_b$) value for the compound is $5.7 \times 10^4$ M⁻¹. The observed binding constant value shows the highest binding affinity [42].
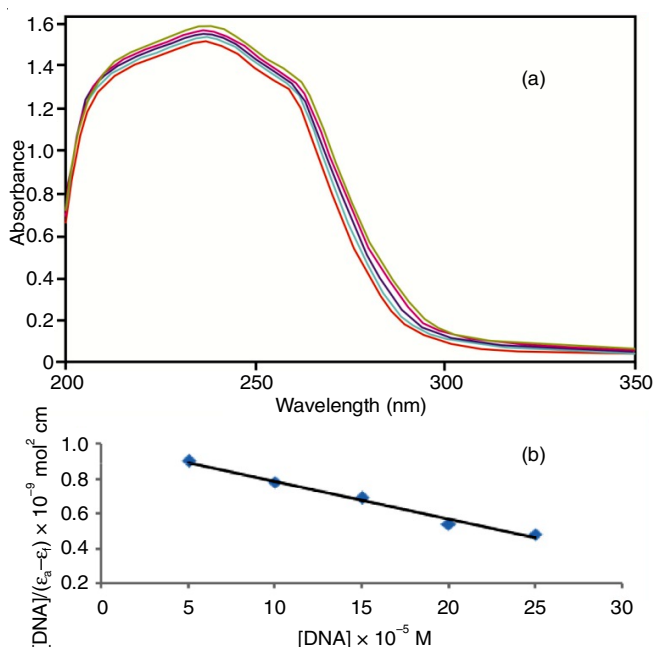


Fig. 6. (a) Absorption trace of copper(II) complex and (b) plot of [DNA]/$\varepsilon_a$–$\varepsilon_f$ *vs*. [DNA]

## REFERENCES

1. K. Butsch, A. Sandleben, M.H. Dokoohaki, A.R. Zolghadr and A. Klein, *Inorganics*, **7**, 53 (2019);
https://doi.org/10.3390/inorganics7040053.
2. L.J. Bourhis, O.V. Dolomanov, R.J. Gildea, J.A.K. Howard and H. Puschmann, *Acta Crystallogr. A*, **71**, 59 (2015);
https://doi.org/10.1107/S2053273314022207.
3. J. Miklovic, D. Valigura, I. Svoboda, J. Moncol and M. Mazur, *Nova Biotechnol. Chem.*, **15**, 190 (2016);
https://doi.org/10.1515/nbec-2016-0019.
4. R.J. Butcher, J.W. Overman and E. Sinn, *J. Am. Chem. Soc.*, **102**, 3276 (1980);
https://doi.org/10.1021/ja00529a079.
5. H. Banerjee, S. Chakraborty and T. Saha-Dasgupta, *Inorganics*, **5**, 47 (2017);
https://doi.org/10.3390/inorganics5030047.
6. E.J. Jung, U.K. Lee and B.K. Koo, *Inorg. Chim. Acta*, **361**, 2962 (2008);
https://doi.org/10.1016/j.ica.2008.01.029.
7. F.-N. Shi, L. Cunha-Silva, T. Trindade, F.A.A. Paz and J. Rocha, *Cryst. Growth Des.*, **9**, 2098 (2009);
https://doi.org/10.1021/cg8004932.
8. M. Tabatabace, R. Mohamadinasab, K. Ghaini and H.R. Khavasi, *Bull. Chem. Soc. Ethiop.*, **3**, 401 (2010).
9. C. Xie, Z. Zhang, X. Wang, X. Liu, G. Shen, R. Wang and D. Shen, *J. Coord. Chem.*, **57**, 1173 (2004);
https://doi.org/10.1080/00958970412331281782.
10. G. D'Ascenzo, A. Marino, M. Sabbatini and T. Bica, *Thermochim. Acta*, **25**, 325 (1979);
https://doi.org/10.1016/0040-6031(78)87008-7.
11. E.E. Sileo, M.A. Blesa, G. Rigotti, B.E. Rivero and E.E. Castellano, *Polyhedron*, **15**, 4531 (1996);
https://doi.org/10.1016/0277-5387(96)00189-1.
12. Z.A. Saddiqi, I.A. Ansari, F. Sama and M. Shahid, *Int. J. Innov. Res. Sci. Eng. Technol.*, **3**, 8673 (2014).
13. H. Park, A.J. Lough, J.C. Kim, M.H. Jeong and Y.S. Kang, *Inorg. Chim. Acta*, **360**, 2819 (2007);
https://doi.org/10.1016/j.ica.2006.12.047.
14. J.R.-H. Xie, V.H. Smith Jr. and R.E. Allen, *J. Chem. Phys.*, **322**, 254 (2006);
https://doi.org/10.1016/j.chemphys.2005.08.040.
15. E.W. Schmidt, Hydrazine and its Derivatives, Wiley: New York (1984).
16. L.F. Audrieth and B.O. Ackerson, The Chemistry of Hydrazine, Wiley: New York (1951).
17. A. I. Vogel, A text Book of Quantitative Inorganic Analysis, Longman: London, edn. 3 (1962).
18. L. Erdey and I. Buzas, Gravimetric Analysis, Part II, Pergamon, London (1965).
19. C.K. Johnson, ORTEP ORNL-3794, Oak Ridge National Laboratory, Tennessee (1976).
20. G.M. Sheldrick, SHELXL-97 program for Crystal Determination, University of Cambridge, England (1977).
21. N.K. Dalley, M.H. Mueller and S.H. Simonsen, *Inorg. Chem.*, **11**, 1840 (1972);
https://doi.org/10.1021/ic50114a020.

22. M. Suenaga, *J. Comput. Chem. Jpn.*, **4**, 25 (2005);
    https://doi.org/10.2477/jccj.4.25.
23. M.A. Spackman and D. Jayatilaka, *CrystEngComm*, **11**, 19 (2009);
    https://doi.org/10.1039/B818330A.
24. F.L. Hirshfeld, *Theor. Chim. Acta*, **44**, 129 (1977);
    https://doi.org/10.1007/BF00549096.
25. H.F. Clausen, M.S. Chevallier, M.A. Spackman and B.B. Iversen, *New J. Chem.*, **34**, 193 (2010);
    https://doi.org/10.1039/B9NJ00463G.
26. A.L. Rohl, M. Moret, W. Kaminsky, K. Claborn, J.J. McKinnon and B. Kahr, *Cryst. Growth Des.*, **8**, 4517 (2008);
    https://doi.org/10.1021/cg8005212.
27. S.K. Wolff, D.J. Grimwood, J.J. McKinnon, D. Jayatilaka and M.A. Spackman, Crystal Explorer 2.0; University of Western Australia: Perth, Australia (2007).
28. W. Williams, M.E. Cuvelier and C. Berset, *LWT-Food Sci. Technol.*, **28**, 25 (1995);
    https://doi.org/10.1016/S0023-6438(95)80008-5.
29. R. Ragul and B.N. Sivasankar, *Inorg. Metal-Org. Nano-Metal Chem.*, **43**, 382 (2013);
    https://doi.org/10.1080/15533174.2012.740736.
30. G.B. Bagihalli, P.G. Avaji, S.A. Patil and P.S. Badami, *Eur. J. Med. Chem.*, **43**, 2639 (2008);
    https://doi.org/10.1016/j.ejmech.2008.02.013.
31. M. Saravanabhavan, K. Sathya, V.G. Puranik and M. Sekar, *Spectrochim. Acta A Mol. Biomol. Spectrosc.*, **118**, 399 (2014);
    https://doi.org/10.1016/j.saa.2013.08.115.
32. M. Saravanabhavan, V. Murugesan and M. Sekar, *J. Photochem. Photobiol.*, **133**, 145 (2014);
    https://doi.org/10.1016/j.jphotobiol.2014.02.020.
33. S. Sathiyaraj, K. Sampath, G. Raja, R.J. Butcher, C. Jayabalakrishnan and S.K. Gupta, *Inorg. Chim. Acta*, **406**, 44 (2013);
    https://doi.org/10.1016/j.ica.2013.07.001.
34. G.H. Cui, T.F. Liu and X. Peng, *J. Chem. Crystallogr.*, **41**, 322 (2011);
    https://doi.org/10.1007/s10870-010-9881-9.
35. A. Braibanti, F. Dallavalle, M.A. Pellinghelli and E. Leporati, *Inorg. Chem.*, **7**, 1430 (1968);
    https://doi.org/10.1021/ic50065a034.
36. K. Nakamoto, Infrared and Raman Spectra of Inorganic and Coordination Compounds, Wiley Interscience: New York, edn 3 (1978).
37. B. Murphy, G. Roberts, S. Tyagi and B.J. Hathaway, *J. Mol. Struct.*, **698**, 25 (2004);
    https://doi.org/10.1016/j.molstruc.2004.02.025.
38. M. Imran, J. Iqbal, S. Iqbal and N. Ijaz, *Turk. J. Biol.*, **31**, 67 (2007).
39. A.A.H. Kadhum, A.B. Mohamad, A.A. Al-Amiery and M.S. Takriff, *Molecules*, **16**, 6969 (2011);
    https://doi.org/10.3390/molecules16086969.
40. Z.-C. Liu, B.-D. Wang, B. Li, Q. Wang, Z.-Y. Yang, T.-R. Li and Y. Li, *Eur. J. Med. Chem.*, **45**, 5353 (2010);
    https://doi.org/10.1016/j.ejmech.2010.08.060.
41. A. Wolfe, G.H. Shimer Jr. and T. Meehan, *Biochemistry*, **26**, 6392 (1987);
    https://doi.org/10.1021/bi00394a013.
42. S. Nafisi, A.A. Saboury, N. Keramat, J.-F. Neault and H.-A. Tajmir-Riahi, *J. Mol. Struct.*, **827**, 35 (2007);
    https://doi.org/10.1016/j.molstruc.2006.05.004.